Approximate solution to predict the enhancement factor for the reactive absorption of a gas in a liquid flowing through a microporous membrane hollow fiber

Kumar, P.S.; Hogendoorn, J.A.; Feron, P.H.M.; Versteeg, G.F.

Published in:
Journal of Membrane Science

DOI:
10.1016/S0376-7388(02)00531-8

Publication date:
2003

ELSEVIER

Journal of Membrane Science 213 (2003) 231–245

journal of MEMBRANE SCIENCE

www.elsevier.com/locate/memsci

Approximate solution to predict the enhancement factor for the reactive absorption of a gas in a liquid flowing through a microporous membrane hollow fiber

P.S. Kumar [a,1], J.A. Hogendoorn [a], P.H.M. Feron [b], G.F. Versteeg [a,*]

[a] *OOIP Group, Faculty of Chemical Technology, University of Twente, P.O. Box 217, 7500 AE Enschede, The Netherlands*
[b] *TNO Environment, Energy and Process Innovation, 7300 AH Apeldoorn, The Netherlands*

Received 16 May 2002; received in revised form 4 November 2002; accepted 6 November 2002

Abstract

Approximate solutions for the enhancement factor (based on the traditional mass transfer theories) for gas–liquid systems with a liquid bulk have been adapted to situations where a liquid bulk may be absent and a velocity gradient is present in the mass transfer zone. Such a situation is encountered during the absorption a gas in a liquid flowing through a hollow fiber. The explicit solution of DeCoursey [Chem. Eng. Sci. 29 (1974) 1867] for a second-order irreversible reaction has been used as a representative sample of the approximate solutions available in literature. It was chosen because of the accuracy of its predictions and the simplicity in use. The solution of DeCoursey was adapted, but still has limitations at long gas–liquid contact times. Under these conditions, the actual driving force for mass transfer of the gas phase species may not be identical for physical and reactive absorption. Also for these situations, there may be a significant depletion of the liquid phase reactant at the axis of the fiber (which is considered to be analogous to the liquid bulk in traditional mass transfer models). A criterion has been proposed for the applicability of the adapted DeCoursey's approximate solution for a second-order irreversible reaction. Within the range of applicability, the approximate solution has been found to be accurate with respect to the exact numerical solution of the mass transfer model as well as the experimentally determined values of enhancement factor in a single hollow fiber membrane gas–liquid contactor. The single hollow fiber membrane contactor that has been used in this study has potential for use as a model gas–liquid contactor. This contactor can thus be used, along with the present approximate solution of the enhancement factor, to obtain the physicochemical properties of a reactive gas–liquid system from the experimental absorption flux measurements or vice versa, as described in the present work.

Keywords: Absorption; Mass transfer; Membrane; Gas–liquid contactor; Enhancement factor

1. Introduction

Microporous hollow fiber membrane modules can be conveniently used for gas–liquid mass transfer operations and offer numerous advantages over conventional contactors like plate and packed columns [1]. The design of membrane gas–liquid contactors is relatively simple and the scale-up is linear because

* Corresponding author. Tel.: +31-53-489-4337; fax: +31-53-489-4774.
E-mail address: g.f.versteeg@ct.utwente.nl (G.F. Versteeg).
[1] Present address: Shell Global Solutions International B.V., P.O. Box 541, 2501 CM The Hague, The Netherlands.

0376-7388/02/$ – see front matter
PII: S0376-7388(02)00531-8

Nomenclature

b	constant in Eq. (3) (dimensionless)
c	constant in Eq. (3) (dimensionless)
C	concentration (mol m^{-3})
$\langle C_{m,L} \rangle$	length averaged mixed cup concentration of A (mol m^{-3})
$C_{m,z}$	mixed cup concentration at z (mol m^{-3})
d	inside diameter of the hollow fiber (m)
d_p	pore diameter (m)
D	diffusion coefficient (m^2 s^{-1})
E	enhancement factor (dimensionless)
E_∞	asymptotic enhancement factor (dimensionless)
Gz	Graetz number, $\langle v \rangle d^2/DL$ (dimensionless)
Ha	Hatta number (dimensionless)
J	local absorption flux (mol m^{-2} s^{-1})
$\langle J \rangle$	length averaged absorption flux (mol m^{-2} s^{-1})
k	mass transfer coefficient (m s^{-1})
$k_{1,1}$	reaction rate constant (m^3 mol^{-1} s^{-1})
k_{ext}	external mass transfer coefficient (m s^{-1})
K_0	constant in Eq. (6) (m)
K_{ov}	overall mass transfer coefficient (m s^{-1})
L	length of the hollow fiber (m)
m	physical solubility ($(C_{A,l}/C_{A,g})_{eq}$) (dimensionless)
M_w	molecular weight (dimensionless)
P	contactor pressure (kPa)
r	distance in radial direction from the axis of hollow fiber (m)
R	radius of the hollow fiber (m)
Re	Reynolds number ($d\langle v \rangle \rho/\mu$) (dimensionless)
R_i	reaction rate (mol m^{-3} s^{-1})
Sc	Schmidt number ($\mu/\rho D$) (dimensionless)
Sh	Sherwood number (kd/D) (dimensionless)
t	time (s)
T	temperature (K)
$\langle v \rangle$	average liquid velocity (m s^{-1})
v_z	liquid velocity in the axial direction (m s^{-1})
z	distance in the axial direction from the liquid inlet (m)

Greek letters

δ	thickness of the membrane (m)
ε	porosity (dimensionless)
ν	stoichiometric coefficient (dimensionless)
τ	tortousity (dimensionless)

Subscripts

app	approximation
A	gas phase species
bulk	bulk phase conditions
Chem	chemical absorption
e	effective
g	gas phase
i	chemical species
in	inlet gas stream
I	gas–liquid interface
K	Knudsen
l	laminar
L	liquid
LM	log mean
m	membrane
num	numerical
out	outlet gas stream
Phys	physical absorption
Plug	plug flow of liquid
z	axial coordinate
0	liquid inlet conditions

Superscript

*	without well-defined liquid bulk

of the modular nature of the contactor. For physical absorption of a gas in a liquid, important contactor specific design parameters are the mass transfer coefficients and the interfacial area for gas–liquid mass transfer. Since the liquid flow through the hollow fiber is laminar, the liquid side mass transfer coefficient can be estimated accurately using approximate solutions or correlations. The interfacial area for mass transfer (which is usually difficult to estimate within a reasonable accuracy for conventional contactors) is easy to determine, as it is simply the membrane surface area.

For well-known reasons, the reactive absorption of a gas in liquid is normally preferred over physical absorption [2]. In the reactive absorption of a gas in a liquid, the contribution of the chemical reaction to the enhancement of the mass transfer rate is traditionally quantified by a term called enhancement factor (E). This parameter needs to be quantified accurately for a good design of the gas–liquid contactor. Depending upon the degree of complexity in describing the absorption process, different approaches have been used by the membrane researchers to estimate the enhancement factor. The simplest approach is to use analytical solutions based on the traditional mass transfer theories described below, which are available for certain asymptotic conditions in the gas–liquid contactor [3,4]. Similarly, an approximate analytical solution of a mass transfer model based on the film theory [5], applicable over a wider range of process conditions has also been used to qualitatively interpret the experimental data [6,7]. It should be noted however that the traditional mass transfer models assume the presence of a well-mixed liquid bulk (relatively large compared to the mass transfer zone) adjacent to the mass transfer zone, which may not be present in case of the absorption of a gas in the liquid flowing through the hollow fiber, especially for small fiber diameters. Also, an additional feature of gas absorption in hollow fiber membranes is the presence of a velocity profile in the liquid side mass transfer zone. In addition to the above mentioned (approximate) analytical solutions, the absorption process in the membrane hollow fibers can be rigorously described using the differential mass balance equations. The exact numerical results of these equations can be used to accurately predict the enhancement factor [8,9].

While a large number of mass transfer models is available in literature to describe the absorption process in gas–liquid systems with a well-defined liquid bulk [10], only three mass transfer models based on the film, penetration and surface renewal theories respectively are widely used to predict the contribution of the chemical reaction in enhancing the mass transfer rate (enhancement factor). Although for a wide range of operating conditions, the film model gives similar enhancement factors as those of the other two models, it is physically unrealistic and should therefore only be chosen because of its ease of use. The penetration and surface renewal models involve unsteady-state diffusion with chemical reaction. As analytical solutions for the above mass transfer models are available for only certain asymptotic conditions, numerical solutions are generally required. Numerical solution of the mass transfer models is usually laborious and complex, necessitating the development of approximate solutions for calculating the enhancement factors based on one of the above mentioned mass transfer models. van Krevelen and Hoftijzer [5] developed an approximate solution for the enhancement factor based on the film theory. Yeramian et al. [11], Hikita and Asai [12] proposed approximate solutions based on Higbie's penetration theory. Onda et al. [13] and DeCoursey [14,15] have provided approximate solutions based on Danckwert's surface renewal theory. It should be noted that the above-cited references for the approximate solutions to various mass transfer theories are only indicative, as considerably more information is available in literature.

In the present work, the applicability and limitations of the approximate solutions for the enhancement factor based on the traditional mass transfer models (with liquid bulk) are explored for their use in the design of membrane gas–liquid contactors (with no liquid bulk). The explicit approximate solution of DeCoursey [14] was used as a test case and the results of it will be compared with the exact numerical results obtained for a membrane hollow fiber. For an irreversible second-order reaction, the approximate results were also compared with the experimental results of a single fiber membrane gas–liquid contactor.

2. Theory

For a situation where a liquid flows inside the non-wetted hollow fibers of a membrane module, the mass transfer of a component A from the gas phase flowing outside the hollow fibers to the liquid can be described by the traditional "resistances in series" model, as given below. Here, a reaction occurs between A and the species B present in the liquid phase:

$$\langle J_A \rangle = K_{ov}\, \Delta C_A \tag{1}$$

Not only in gas–liquid systems with liquid bulk, but also in membrane gas absorption processes, the overall

mass transfer coefficient (K_{ov}) is generally expressed as follows [8]:

$$\frac{1}{K_{ov}} = \frac{1}{k_g} + \frac{1}{k_m} + \frac{1}{mk_L E} \quad (2)$$

The gas side mass transfer coefficient, k_g depends on the fluid hydrodynamics in the "shell side" of the membrane module and is module specific due to the high packing density and non-uniform spacing of the hollow fibers within the membrane module [1]. This may result in maldistribution of the gas flow around the fibers (like channeling). A number of correlations of the form of Eq. (3) to predict k_g, based on dimensionless numbers, is available in literature [1]:

$$Sh_g = b(Re_g)^c(Sc_g)^{0.33} \quad (b \text{ and } c \text{ are constants}) \quad (3)$$

Assuming that there is no convective transport of A through the microporous membrane, the mass transfer across the membrane can be described using Fick's law and the mass transfer coefficient related to the transport process through the membrane can be defined as

$$k_m = \frac{D_{A,e}}{\delta} = D_A \frac{\varepsilon}{\delta\tau} \quad (4)$$

Depending upon the pore diameter (d_p) of microporous membrane and the gas phase pressure, the diffusion through the pores can be due to bulk diffusion ($d_p > 1.0\times10^{-5}$ m) or Knudsen diffusion ($d_p < 1.0\times10^{-7}$ m) or both in the intermediate region. A detailed description on the mass transport process through a microporous membrane can be found elsewhere [16]. For a binary gas mixture, the diffusion coefficient, D_A in a porous structure is calculated as given below:

$$\frac{1}{D_A} = \frac{1}{D_{A,j}} + \frac{1}{D_{K,A}} \quad (5)$$

The Knudsen diffusion coefficient is given by

$$D_{K,A} = K_0\sqrt{\frac{8RT}{\pi M_w}} \quad (6)$$

For a (ideal) membrane with cylindrical pores, K_0 is equal to $4\varepsilon d_p/3\tau$. In reality, the parameter K_0 depends on the morphology of the membrane and the interaction between the molecules and porous structure. For single gas permeation, the values of K_0 for various commercial polyolefin membranes and gases respectively were experimentally determined by Guijt et al. [17]. The bulk diffusion coefficient can be calculated from the kinetic theory of gases. The liquid side mass transfer coefficient can be obtained from Leveque's solution derived from the analogous case of Graetz's heat transfer problem of laminar flow of a liquid through a circular duct [18]. The assumptions involved in Leveque's solution are constant gas–liquid interface conditions and a fully developed laminar flow of liquid through the fiber. The following correlations are available for the asymptotic regions of the Graetz number (Gz):

$$\text{for } Gz < 10, \quad Sh_L = 3.67 \quad (7)$$

$$\text{for } Gz > 20, \quad Sh_L = 1.62(Gz)^{1/3} \quad (8)$$

Kreulen et al. [19] presented a correlation valid over the entire range of Graetz numbers (Gz):

$$Sh = \frac{k_L d}{D_A} = \sqrt[3]{3.67^3 + 1.62^3 Gz} \quad (9)$$

The above correlations (7–9) are based on the following definition of the average mass transfer coefficient, k_L:

$$k_L = \frac{\langle J_A\rangle}{(C_{A,l} - \langle C_{m,L}\rangle)} \quad (10)$$

where $\langle C_{m,L}\rangle$ is the mixing cup (analogous to average bulk) concentration of A averaged over the length of the hollow fiber. For laminar flow of liquid through a hollow fiber, with a fully developed velocity profile, the mixing cup concentration of A in the liquid, at any axial distance, z from the liquid inlet side of the fiber is as follows [19]:

$$C_{m,z} = C_{A,l}\left[1 - \exp\left(-\frac{4k_L z}{\langle v\rangle d}\right)\right] \quad (11)$$

The average bulk concentration of A ($\langle C_{m,L}\rangle$) in the fiber can be obtained from the integration of $C_{m,z}$ over the length of the fiber:

$$\langle C_{m,L}\rangle = \frac{C_{A,l}}{L}\left\{L + \frac{\langle v\rangle d}{4k_L}\left[\exp\left(-\frac{4k_L L}{\langle v\rangle d}\right) - 1\right]\right\} \quad (12)$$

The enhancement factor E that describes the influence of a chemical reaction on the mass transfer rate in Eq. (2) can be obtained either from the exact numerical solution of the mass transfer models or

analytical/approximate solutions of the mass transfer models. The enhancement factor affects the mass transfer rate significantly and thus the design of membrane gas–liquid contactors and will be the subject of further discussion.

3. Numerical model

For the reactive absorption of a gas in a liquid flowing through a microporous hollow fiber, the differential mass balance for any species, i, present in the liquid phase is given by

$$v_z \frac{\partial C_i}{\partial z} = D_i \left[\frac{1}{r} \frac{\partial}{\partial r} \left(r \frac{\partial C_i}{\partial r} \right) \right] - R_i \tag{13}$$

In arriving at Eq. (13), the diffusion in axial direction was neglected and axi-symmetry of the hollow fiber was assumed. The temperature effect during the absorption process was considered to be negligible. Since the liquid flow inside the fiber is laminar, the velocity profile in the radial direction is given by

$$v_z = 2\langle v \rangle \left[1 - \left(\frac{r}{R} \right)^2 \right] \tag{14}$$

For a hypothetical situation where a gas is absorbed in a liquid flowing through a fiber under plug flow conditions, the differential mass balance Eq. (13) reduces to the following form:

$$\frac{\partial C_i}{\partial t} = D_i \left[\frac{1}{r} \frac{\partial}{\partial r} \left(r \frac{\partial C_i}{\partial r} \right) \right] - R_i, \quad \text{where } t = \frac{z}{\langle v \rangle} \tag{15}$$

This is similar to the unsteady-state mass balance equation of the penetration theory described in cylindrical coordinates and the important physical difference in the present case is the absence of a well-mixed bulk as described earlier. In this work, an irreversible second-order reaction of the following type was assumed to occur in the liquid phase:

$$\mathrm{A} + \nu_\mathrm{B}\mathrm{B} \Rightarrow \mathrm{C} + \mathrm{D} \tag{16}$$

The partial differential Eq. (13) (laminar flow) and Eq. (15) (plug flow) require the following initial and boundary conditions in the axial and radial directions respectively and they are described in detail by Kreulen et al. [8]:

$$\text{at } z = 0, \quad \text{for all } r, \quad C_i = C_{i,0} \tag{17}$$

$$\text{at } r = 0, \quad \text{for } z > 0, \quad \left(\frac{\partial C_i}{\partial r} \right) = 0 \tag{18}$$

$$\text{at } r = R, \quad \text{for } z > 0, \quad \left(\frac{\partial C_i}{\partial r} \right)_{i \neq \mathrm{A}} = 0 \tag{19}$$

$$D_\mathrm{A} \left(\frac{\partial C_i}{\partial r} \right) = k_\mathrm{ext} (C_{\mathrm{A,g,bulk}} - C_{\mathrm{A,g,l}}) \tag{20}$$

The external mass transfer coefficient (k_ext) is a lumped parameter comprising of the resistances to mass transport of species A due to the gas phase and microporous membrane:

$$\frac{1}{k_\mathrm{ext}} = \frac{1}{k_\mathrm{g}} + \frac{1}{k_\mathrm{m}} \tag{21}$$

The set of partial differential equations (the number depends on the number of chemical species involved in the reaction scheme) was solved numerically using a technique similar to the one described by Versteeg et al. [20]. In the numerical solution of the differential equations, the value of k_ext was kept very high ($10^6\ \mathrm{m\,s^{-1}}$) to focus completely on the mass transfer with chemical reaction occurring in the liquid phase (by neglecting the resistance due to the membrane and gas phase). The concentration profile of the absorbed gas (A) in the liquid phase was obtained from the solution of the mass balance equations. The local absorption flux of A along the length of the fiber was subsequently calculated using Fick's law. The average absorption flux ($\langle J_\mathrm{A} \rangle$) was obtained from the integration of the local fluxes along the length of the fiber:

$$\langle J_\mathrm{A} \rangle = \frac{1}{L} \int_0^L J_\mathrm{A}(z)\, \mathrm{d}z \tag{22}$$

The exact numerical enhancement factor (E) is defined as the ratio of the absorption rate/flux of a gas in the liquid in the presence of a chemical reaction to the absorption rate/flux in the absence of a reaction:

$$E_\mathrm{num} = \frac{\langle J_{\mathrm{A,Chem}} \rangle_\mathrm{num}}{\langle J_{\mathrm{A,Phys}} \rangle_\mathrm{num}} \tag{23}$$

It should be noted that the above definition for the enhancement factor traditionally applies to a situation where the driving force (of A) for mass transfer is identical in the presence and absence of a chemical reaction. However, the above conditions may not be satisfied for large gas–liquid contact time in a membrane contactor (or at low Graetz numbers). In these

situations, there will be a significant concentration ($\langle C_{m,L} \rangle$) of A in the liquid "bulk" for the case of physical absorption (Eq. (12)). Nevertheless, this definition will be used to calculate the overall enhancement factor for a membrane contactor and instead the enhancement factor predicted by the approximate solutions of traditional mass transfer models will be adapted to incorporate the change in the concentration of A in the liquid "bulk".

4. Approximate solutions for enhancement factor

Numerous approximate solutions to the earlier described mass transfer models are available in the literature that are applicable over a wide range of process conditions, reactions of differing complexity and chemical solute loadings. However, all the models assume the presence of a well-mixed liquid bulk adjacent to the mass transfer zone and therefore the dimensionless Hatta number and infinite enhancement factor used in these approximate solutions are based on the conditions existing in the liquid bulk. Depending upon the gas–liquid contact time, the mass transfer zone in the liquid phase of the hollow fiber may actually extend up to the axis of the fiber and the centerline concentration may be disturbed. Under the limiting condition of short gas–liquid contact time, the penetration depth of the gas phase species diffusing from the gas–liquid interface is small in comparison to the fiber radius. Consequently, the liquid far from the interface (say at the axis of the fiber) is essentially undisturbed (analogous to the liquid bulk that is assumed to be present at infinite distance from the gas–liquid interface in traditional mass transfer models) and the concentration of the liquid phase reactant B at the centerline (axis) is the same as the concentration of B in the liquid entering the fiber. For that case, the dimensionless Hatta number and asymptotic enhancement factor, adopted for a hollow fiber can be described based on the conditions at the liquid inlet ($z = 0$):

$$\text{Hatta number}: \quad Ha^* = \frac{\sqrt{k_{m,n} D_A C_{A,l}^{m-1} C_{B,0}^{n}}}{k_L} \tag{24}$$

where m and n are the partial reaction order with respect to A and B respectively. The mass transfer coefficient for the laminar flow conditions was estimated using the Leveque's solution (Eqs. (7)–(9)). For plug flow of liquid through the hollow fiber, k_L was estimated using the following equation [10]:

$$k_{L,\text{Plug}} = 2\sqrt{\frac{D_A}{\pi \tau}} = 2\sqrt{\frac{D_A L}{\pi \langle v \rangle}} \tag{25}$$

The asymptotic infinite enhancement factor for an irreversible reaction is defined as

$$E_\infty^* = \left(1 + \frac{C_{B,0} D_B}{v_B m C_{A,g,l} D_A}\right) \left(\frac{D_A}{D_B}\right)^q \tag{26}$$

The above definition neglects the drift/convective flow caused by the diffusion of solute gas, A. This is in line with the assumptions associated with the Fick's law, which is the basis for the definition. The value of q varies depending upon the type of mass transfer model chosen and is given below:

film model : $q = 0$

penetration model : $q = \frac{1}{2}$

Leveque model (presence of a velocity gradient in the mass transfer zone) : $q = \frac{1}{3}$

In the present work, the applicability and limitations of using an approximate solution of one of the mass transfer models (all developed originally for the case where a well-defined liquid bulk is present) to predict the enhancement factor for the reactive absorption of a gas in a liquid flowing through a hollow fiber were investigated. The explicit approximate solution of DeCoursey based on Danckwert's surface renewal theory, developed originally for an irreversible second-order chemical reaction [14], was used as an example:

$$E_{\text{app}} = \frac{-(Ha^*)^2}{2(E_\infty^* - 1)} + \sqrt{\left[\frac{(Ha^*)^2}{4(E_\infty^* - 1)^2} + \frac{E_\infty^* (Ha^*)^2}{(E_\infty^* - 1)} + 1\right]} \tag{27}$$

DeCoursey [15] later extended the above expression to a reversible reaction that is second-order in both directions and for equal diffusivities of reactants and products. The definition of the infinite enhancement factor (E_∞) was suitably modified for a reversible reaction. Later, DeCoursey and Thring [21] presented

an implicit expression for the enhancement factor for a reversible reaction and unequal diffusivities of reactants/products. Recently, Hogendoorn et al. [22] have shown that with a suitable adaptation for E_∞, Eq. (27) can be used to predict the enhancement factor for a reversible reaction of finite rate and unequal diffusivity of reactants. An adapted analytical solution for the infinite enhancement factor for film model as derived by Secor and Beutler [23] for an instantaneous reversible reaction, was used by the authors to calculate E_∞. To conclude, though the present work is based on Eq. (27) for an irreversible reaction type of (16), it can be easily extended to other situations in line with the work of Hogendoorn et al. [22].

The approximate solution for the enhancement factor (E_{app}) is usually obtained by developing an approximate solution for the time averaged (in the present case length averaged) absorption flux ($\langle J_{A,Chem}\rangle_{app}$) in the presence of a chemical reaction. Further, E_{app} is obtained as per definition by dividing $\langle J_{A,Chem}\rangle_{app}$ by the time/length averaged absorption flux in the absence of a chemical reaction. For an unloaded solution:

$$\langle J_{A,Phys}\rangle_{app} = k_L C_{A,l} \tag{28}$$

The enhancement factor as per the traditional definition is (for $C_{A,bulk} = 0$):

$$E_{app} = \frac{\langle J_{A,Chem}\rangle_{app}}{k_L C_{A,l}} \tag{29}$$

However, the Leveque solution that provides an accurate estimate of k_L for the mass transfer in a hollow fiber is related to the absorption flux according to Eq. (10). For physical absorption, the effective driving force for the mass transfer of A is reduced for long gas–liquid contact time, due to the saturation of the liquid by the gas absorbed. Therefore, the traditional approximate solutions for the enhancement factor available in the literature, which assume a negligible concentration of A in the liquid bulk, need to be adapted to the present situation to enable a proper comparison with the exact numerical solution:

$$E_{app,l} = E_{app}\frac{C_{A,l}}{(C_{A,l} - \langle C_{m,L}\rangle)} \tag{30}$$

For large Graetz numbers (Gz), the saturation of the liquid by the solute gas is insignificant ($C_{A,l} \gg \langle C_{m,L}\rangle$). Therefore,

$$E_{app,l} = E_{app} \tag{31}$$

It should be remembered that Eq. (27) is an approximate solution for the penetration model in rectangular coordinates and therefore its simple extension to the present case (cylindrical geometry) essentially means that the curvature effects were neglected.

5. Experimental setup and procedure

The reactive absorption of a gas in a liquid flowing through a hollow fiber was studied in a single fiber membrane gas–liquid contactor. The schematic diagram of the membrane contactor is shown in Fig. 1. The details regarding the experimental setup can be obtained from Kumar et al. [9]. A microporous polypropylene hollow fiber (Accurel PP: type Q3/2; average pore diameter: 0.2 mm; d_{in}: 600 mm) was used in the membrane contactor. Two modes of gas–liquid contacting operation, namely the semi-batch and continuous mode, were studied in the present work. The liquid flow through the hollow fiber was continuous in both modes. In the semi-batch mode, pure gas present outside the hollow fiber was absorbed in the liquid flowing through the fiber. The gas phase pressure outside the hollow fiber was maintained constant by feeding pure gas from a supply vessel to the membrane contactor via a pressure regulator. From the drop in gas pressure in the supply vessel, the gas absorption rate/flux was calculated. In the continuous mode, a gas stream of known composition was fed to the membrane contactor and the composition of the gas stream entering and leaving the contactor was measured using an infrared (IR) gas analyzer. The gas stream (CO_2/N_2) flowed concurrent with respect to the liquid flow direction. By making a mass balance over the gas phase of the membrane contactor, the

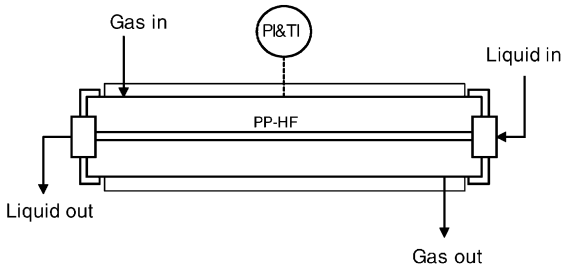

Fig. 1. Experimental single fiber membrane gas–liquid contactor.

absorption rate/flux was calculated. Further information about the experimental procedure can be obtained in Kumar et al. [9]. The accuracy of the experimental setup was tested by measuring the physical absorption flux of N_2O and CO_2 in water. For physical absorption, the solubility (m) and diffusion coefficient (D_A) of the gas in liquid are the required (absorption) system specific input parameters for the numerical model and accurate information on these parameters is available in literature [24]. Therefore, the numerical model should provide an accurate prediction of the absorption flux if compared to the experimental data. The absorption of CO_2 in aqueous NaOH solutions was used as a model reactive system, as accurate information on the physicochemical parameters of this system is available in literature and the reaction also fits into the reaction scheme given by (16).

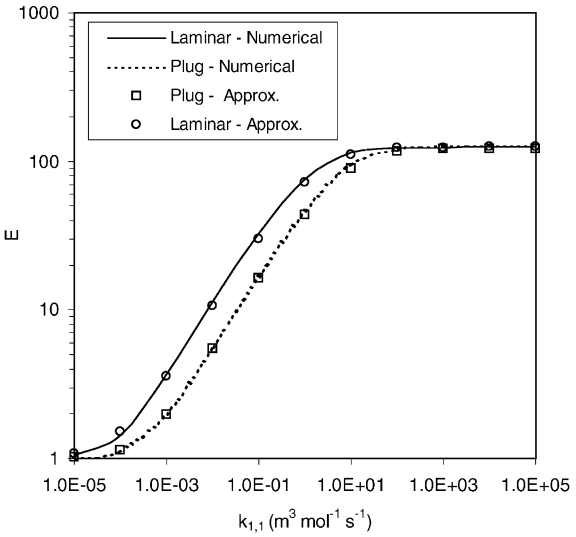

Fig. 2. The influence of the reaction rate constant on the enhancement factor for a second-order irreversible reaction (Eq. (16)). Simulation conditions: $L = 0.38\,\text{m}$; $d = 600 \times 10^{-6}\,\text{m}$; $\langle v \rangle = 0.5\,\text{m s}^{-1}$; $C_{A,0} = 41.6\,\text{mol m}^{-3}$; $C_{B,0} = 5000\,\text{mol m}^{-3}$; $D_A = D_B = 1 \times 10^{-9}\,\text{m}^2\,\text{s}^{-1}$; $m = 1.0$; $\nu_B = 1.0$.

6. Results and discussion

6.1. Comparison of the exact numerical solution and approximate solution for the enhancement factor

It should be noted that the DeCoursey's approximate solution is based on the surface renewal theory while the numerical model (at least for the situation where the liquid flow is plug) is related to the penetration theory. However, the difference in the prediction of E between the numerical model and approximate solution based on the two different theories is <2% for an irreversible first-order reaction [20] and <6% for an irreversible second-order reaction with equal diffusivities of the reactants [14]. Fig. 2 shows the enhancement factor predicted by the DeCoursey equation (adapted as per Eq. (30)) as well as the numerical model for the reactive absorption of a gas in liquid, flowing under plug and laminar conditions inside the hollow fiber as a function of the reaction rate constant. To avoid disturbance in the centerline concentration of A and B, the average residence time of the liquid was kept small enough to have an identical driving force of A for physical and chemical absorption (so that $E_{app,l}$ is identical to E_{app}). The predictions of the approximate solution were in good agreement (within ±5.5% for plug flow and ±7.45% for laminar flow) with the exact solutions of the numerical model (percentage error $= ((E_{num} - E_{app,l})/E_{num}) \times 100$). The larger error for the laminar flow conditions is perhaps due to the error introduced by Leveque's solution (basically a correlation) in the prediction of the mass transfer coefficient for a situation where there is a velocity gradient in the mass transfer zone. The mass transfer coefficient (k_L) predicted by the Leveque solution for asymptotic conditions (Eqs. (7) and (8)) is within ±2% of the exact numerical solution of the mathematical model (for the situation where there is no chemical reaction) described in Section 3. The difference in E for the two flow conditions, at identical reaction rate constant, is due to the difference in the hydrodynamics of the mass transfer zone (presence and absence of a velocity gradient in the liquid) or more specifically on the numerical value of the mass transfer coefficient (k_L). These can be calculated for the two situations using Eqs. (7), (8) and (25) respectively.

For short gas–liquid contact time as considered in the above simulations, the mass transfer zone is thin and is restricted to the gas–liquid interface and therefore, there should be a negligible error due to the curvature of the fiber. This can be observed from similar values of the maximum error of the approximate solution for the present case (5.5% for plug flow and

7.5% for laminar flow) and the errors reported in literature for the penetration model (6%) in rectangular coordinates [14].

While a number of plots similar to Fig. 2 can be generated for laminar flow conditions using the numerical model and approximate solutions, one can find a remarkable similarity between Fig. 2 and the traditional E versus Ha plots. In fact, changing the reaction rate constant in Fig. 2 is the same as changing the Ha^* for a given E^*_∞. Fig. 3 shows the more generalized E versus Ha^* plot based on DeCoursey's approximate solution as well as the numerical results for the case of laminar flow of liquid through the fiber. The Ha^* and E^*_∞ numbers were calculated using the definitions given by Eqs. (24) and (26), respectively. The Ha^* for a given E^*_∞ was varied by changing the second-order reaction rate constant, $k_{1,1}$ and E^*_∞ itself was changed by varying the concentration of the reactant, B in the liquid phase. The accuracy of the enhancement factor predicted by the adapted DeCoursey's approximate solution is within ±8.2% of the exact numerical solution of the model equations. As can be expected,

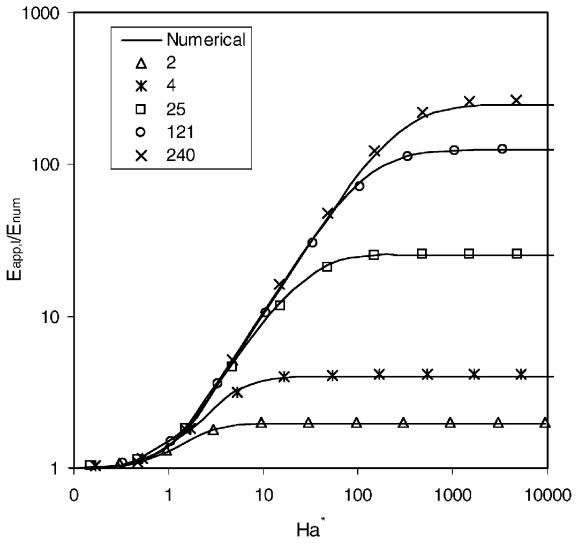

Fig. 3. E vs. Ha^* plot for the absorption of a gas in liquid (laminar flow) of finite depth accompanied by an irreversible second-order reaction (Eq. (16)). Simulation conditions: $L = 0.38$ m; $d = 600\times10^{-6}$ m; $\langle v\rangle = 0.5\,\mathrm{m\,s^{-1}}$; $C_{A,0} = 41.6\,\mathrm{mol\,m^{-3}}$; $C_{B,0} =$ 40–9940 $\mathrm{mol\,m^{-3}}$; $k_{1,1} = 1\times10^{-5}$ to $1\times10^{5}\,\mathrm{m^3\,mol^{-1}\,s^{-1}}$; $D_A = D_B = 1\times10^{-9}\,\mathrm{m^2\,s^{-1}}$; $m = 1.0$; $\nu_B = 1.0$. The legends of the figure indicate the value of E^*_∞ for the conditions used in the numerical simulations as well as in the calculation of $E_{app,1}$.

the maximum error is in the transition region of Ha^* between the asymptotic absorption regimes [such as "$E = Ha^*$" (fast, $2 < Ha^* < E^*_\infty$) and "$E = E^*_\infty$" (instantaneous, $2 < Ha^* > E^*_\infty$)]. In the asymptotic absorption regimes, the approximate solution reduces to the analytical solution of the mass transfer model and therefore the errors of the approximate solutions are minimal in the asymptotic regimes. Though the remarkably accurate prediction of E by the DeCoursey's solution is well known for the situation where a liquid bulk is present [14,22], the accuracy in the present case is also related to the accuracy of the Leveque solution in describing the physical mass transfer process for laminar flow conditions.

6.2. Influence of Graetz number on the applicability of the approximate solutions

6.2.1. 1,1 irreversible reaction, laminar flow; $D_A = D_B = 1\times10^{-9}\ m^2\ s^{-1}$; $\nu_B = 1$

The Graetz number ($\langle v\rangle d^2/D_A L$) is simply the ratio of the penetration time of the solute gas to reach the axis of the hollow fiber (from the gas–liquid interface), to the average residence time of the liquid in the fiber. The influence of Gz on the accuracy of the approximate solution was studied using the parameters shown in Table 1. For low Graetz numbers, there is a significant concentration of A ($\langle C_{m,L}\rangle$) in the liquid "bulk" during physical absorption and in case of a moderate to fast reaction, the concentration of B at the axis of the hollow fiber is less than that of the inlet concentration due to depletion. The consequences due to this are as follows:

1. Due to a significant concentration of A at the centerline incase of physical absorption, the driving force for mass transfer is not necessarily the same

Table 1
Numerical values of the parameters used in the simulations

Parameters	Numerical value
L (m)	0.4
d (m)	600×10^{-6}
$\langle v\rangle$ ($\mathrm{m\,s^{-1}}$)	0.01–2.0
$C_{A,g}$ ($\mathrm{mol\,m^{-3}}$)	41.6
$C_{B,0}$ ($\mathrm{mol\,m^{-3}}$)	10 to 10^4
$k_{1,1}$ ($\mathrm{m^3\,mol^{-1}\,s^{-1}}$)	10^{-3} to 10^3
m	1.0

for physical and reactive absorption, which makes the traditional definition of the enhancement factor rather trivial. However, the traditional approximate solution can be corrected to some extent using Eq. (30) to have a proper basis for the comparison with the exact numerical solutions.

2. The Hatta number and infinite enhancement factor are based on the concentration of B at the liquid inlet ($C_{B,0}$) assuming that the concentration of B at the axis of the hollow fiber is the same as that of $C_{B,0}$. Due to depletion of B, the actual "bulk" concentration of B that should be used in Ha^* and E^*_∞ is less than $C_{B,0}$.

For $Gz > 100$, the values of $E_{app,l}$ were within ±9.1% of the values predicted numerically. As can be expected, the error in the prediction of the approximate solution was relatively high at low Graetz numbers ($Gz < 100$) and the error increased rather exponentially for $Gz < 20$ (see Fig. 4 in which the absolute errors as function of the Gz number are given for a few simulation conditions as examples). This is mostly due to a significant depletion of the concentration of B at the axis of the fiber. The numerical simulations indicated that the minimum value of Gz at which the concentration of the reactant, B is unaltered at the axis and end of the fiber was approximately 120:

$$Gz > 120 \tag{32}$$

On substituting the above number in the Leveque's equation:

$$Sh^*_L = 1.62(Gz)^{1/3} > \cong 8 \tag{33}$$

The above criterion on the applicability of the approximation (based on the Sherwood number) is in line with the criterion proposed by van Elk [25] for gas absorption in a falling liquid film, a similar physical situation where a well-defined liquid bulk is absent. Though the approximate solution is applicable for $Gz > 120$, it could nevertheless be used for values much lower than this without a significant loss of accuracy. As an example, for the range of process conditions mentioned in Table 1, the maximum error in the prediction of the $E_{app,l}$ for Gz equal to 45 was 21%.

For certain asymptotic conditions, the error in the prediction of the approximate solution can be reduced significantly by also making simple corrections to account for the depletion in the concentration of B at the axis of the fiber. For a condition in which the absorption rate of A is limited by the diffusion of the reactant species ($2 < Ha^* \gg E^*_\infty$), the depletion of B can be approximately related to the saturation of A (in the absence of a chemical reaction). Especially at very low Graetz numbers and for instantaneous reactions, the average "bulk" concentration of A, $\langle C_{m,L} \rangle$ in the liquid can be related to the average reduced "bulk" concentration of B, $\langle C_B \rangle$:

$$\frac{\langle C_B \rangle}{C_{B,0}} \cong \frac{C_{A,l} - \langle C_{m,L} \rangle}{C_{A,l}} \tag{34}$$

$\langle C_{m,L} \rangle$ can be calculated using Eq. (12). The adapted average "bulk" concentration, $\langle C_{B\rangle}$ can now be used instead of $C_{B,0}$ to calculate Ha^* and E^*_∞ and hence the enhancement factor. As an example, Fig. 4 shows a few cases in which the correction for the "bulk" concentration of B has been implemented in the approximate solution for the instantaneous absorption regime ($2 < Ha^* \gg E^*_\infty$). As the k_L increases with increase in Graetz number, the Ha^* decreases and the absorption regime gradually shifts away from the instantaneous regime. Consequently, the correction for the "bulk" concentration of B is found to be less suitable for high Gz numbers.

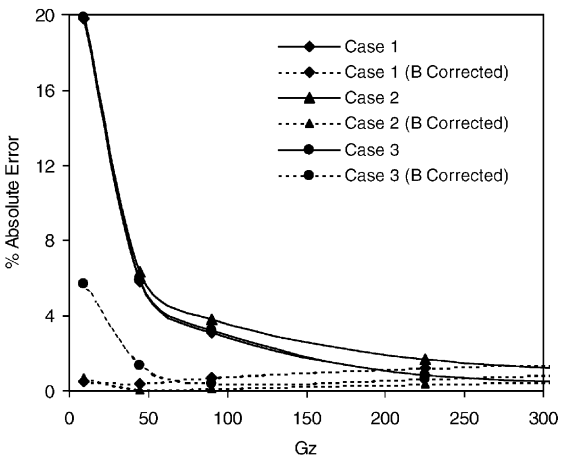

Fig. 4. The influence of the correction of "bulk" concentration of B using Eq. (34) for the 'instantaneous absorption' regime ($2 < Ha* \gg E^*_\infty$). Simulation conditions: $L = 0.4\,m$; $d = 600 \times 10^{-6}\,m$; $\langle v \rangle = 0.01$–$1.5\,m\,s^{-1}$; $C_{A,0} = 41.6\,mol\,m^{-3}$; $D_A = D_B = 1 \times 10^{-9}\,m^2\,s^{-1}$; $m = 1.0$; $\nu_B = 1$. Case 1: $C_{B,0} = 1000\,mol\,m^{-3}$; $k_{1,1} = 10\,m^3\,mol^{-1}\,s^{-1}$. Case 2: $C_{B,0} = 1000\,mol\,m^{-3}$; $k_{1,1} = 100\,m^3\,mol^{-1}\,s^{-1}$. Case 3: $C_{B,0} = 100\,mol\,m^{-3}$; $k_{1,1} = 1\,m^3\,mol^{-1}\,s^{-1}$.

6.2.2. 1,1 irreversible reaction, $D_A/D_B \neq 1$; $\upsilon_B = 1$

In the absence of a velocity gradient in the mass transfer zone, DeCoursey [14] has shown that the approximate solution can be used for values of (D_B/D_A) other than one, with a maximum error of 9%. Though the present case is not identical to the above-described physical situation, the DeCoursey solution can still be conveniently used to predict the enhancement factor. Fig. 5 shows the dimensionless concentration of B at the axis ($r = 0$) and end ($z = L$) of the fiber, for different values of D_B/D_A. Based on this information, the following empirical criterion provides the minimum value of the Graetz number above which the concentration of reactant B is undisturbed at the axis of the hollow fiber and the approximate solution can be used to predict the enhancement factor accurately:

$$Gz > 120\left(\frac{D_B}{D_A}\right) \tag{35}$$

Expressing the criterion in terms of the Sherwood number:

$$Sh_L^* = \frac{k_L R}{D_A} > 4\left(\frac{D_B}{D_A}\right)^{1/3} \tag{36}$$

In contrast to the above criterion, for the absorption of a gas in a falling liquid film, van Elk [25] proposed a 0.5 power dependence of the Sherwood number on the ratio of diffusivities. For the instantaneous absorption regime ($2 < Ha^* \gg E_\infty^*$), Eq. (34) can be used to account for the depletion in the "bulk" concentration of B, to reduce the error in the prediction of E by the adapted approximate solution.

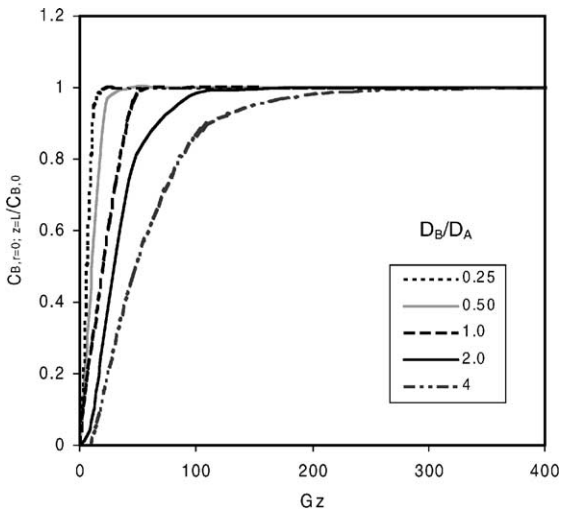

Fig. 5. Dimensionless concentration of B at the axis of the hollow fiber and z equal to L. Simulation conditions: $L = 0.4$ m; $d = 600 \times 10^{-6}$ m; $\langle v \rangle = 0.01$–$1.5\ m\ s^{-1}$; $C_{A,0} = 41.6\ mol\ m^{-3}$; $C_{B,0} = 1000\ mol\ m^{-3}$; $k_{1,1} = 1.0\ m^3\ mol^{-1}\ s^{-1}$; $D_A = 1 \times 10^{-9}\ m^2\ s^{-1}$; $m = 1.0$; $\nu_B = 1.0$.

While the present discussion is restricted to an irreversible second-order reaction, the approximate solutions (DeCoursey solution, as in the present case) can be extended to other situations (like reversible reactions) as dealt with in detail by Hogendoorn et al. [22] for systems with a well-defined liquid bulk. However, necessary criteria (like Eqs. (32) and (35)) to determine the range of applicability of the approximate solutions under various conditions need to be developed.

6.3. Comparison of the experimental enhancement factor (E_{exp}) with the prediction of DeCoursey's approximation solution ($E_{app,l}$)

Based on the conclusions drawn from the discussions in the previous sections, the following experimental conditions were used in the single fiber membrane contactor to satisfy the assumptions/criteria (for applicability) used in the adaptation of the traditional approximate solution for the estimation of the enhancement factor in a hollow fiber.

1. Constant gas–liquid interface conditions (semi-batch mode) (see also Section 2).
2. The range of the liquid velocity was chosen such that the criterion given by Eq. (35) was satisfied.

However, some experiments were also carried out relaxing the above criteria to verify its effect on the error between the $E_{app,l}$, predicted by the adapted approximate solutions and E_{exp}, the experimental enhancement factor. As mentioned earlier, absorption of CO_2 in an aqueous NaOH solution was used as a model reactive system. The physicochemical data used for the calculation of the approximate enhancement factor were obtained from the references given in Table 2. The D_B (mean ion diffusivity of NaOH at infinite dilution) was calculated using the Nernst–Hartley equation. The influence of ionic strength of the aqueous NaOH solution on the reaction rate constant, $k_{1,1}$ was accounted.

In the semi-batch experiments, the physical absorption flux of N_2O/CO_2 in water was measured at 295 K

Table 2
Literature source of the physicochemical data used in the calculation of $E_{app,1}$

Property	System	Literature source
D_A (m)	CO_2–water	[24]
D_A (m)	N_2O–water	[24]
m	CO_2–aqueous NaOH	[27]
D_A	CO_2–aqueous NaOH	[28]
D_B	CO_2–aqueous NaOH	[29]
$k_{1,1}$	CO_2–aqueous NaOH	[30]

and these experimental values were found to be within ±4% of the values predicted by the numerical model. This indirectly gives an indication of the accuracy of the experimental measurements (or setup). Some of the experimental results have already been reported in Kumar et al. [9]. Similarly, the reactive absorption of CO_2 in aqueous NaOH solutions was measured for four different experimental conditions as described in Table 3. For all the experimental data sets, the absorption temperature was maintained at 295±0.2 K and the experimental Graetz number range is given in Table 3. Except for the experimental data set 3, the error in the prediction of $E_{app,1}$ by the present approximate solution was somewhat higher at low Graetz numbers (see Table 3) and it falls in line with the error behavior of the approximate solution as compared to the numerical model (as discussed in Section 6.2). It should be noted that the reproducibility of the experimental data was within ±5%. Due to the experimental conditions used for the semi-batch experiments, the numerical values of the Hatta number and infinite enhancement factor were such that the absorption was in the instantaneous regime ($2 < Ha^* > E^*_\infty$). Therefore, the correction for the depletion in the "bulk" concentration of B as given by Eq. (34) was used. Fig. 6 shows the parity plot of the values of experimental and approximate enhancement factor ($E_{app,1}$) for the four sets of experiments. Here, the corrected or reduced "bulk" concentration of B was used in calculating, $E_{app,1}$. The $E_{app,1}$ predicted by the approximate solution was within ±10.7% (maximum error) of the experimental values of enhancement factor and the average error was 5.4% (see also Table 4).

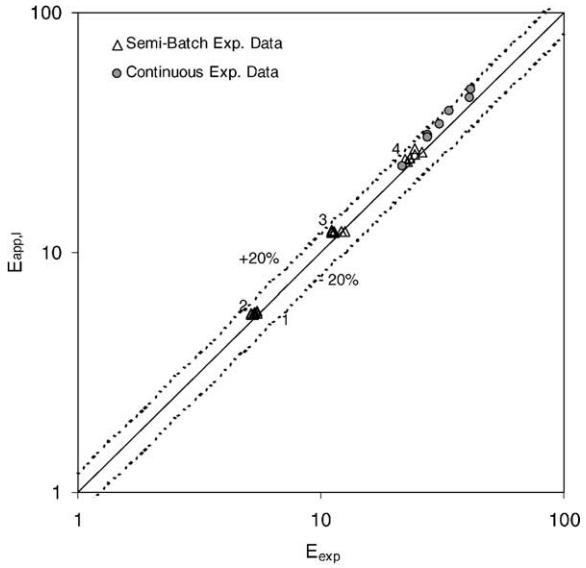

Fig. 6. Parity plot for the experimental and approximate enhancement factor for the absorption of CO_2 in aqueous NaOH solutions. Refer to Tables 3 and 4 for the experimental conditions. The "bulk" concentration of B, used in $E_{app,1}$ has been corrected for the depletion as per Eq. (34), for $Gz < 120(D_B/D_A)$.

Table 3
Experimental conditions for the data provided in the parity plot (semi-batch mode of operation)

Experiment set no.	L (m)	$C_{NaOH,0}$ (mol m^{-3})	$C_{CO_2,g}$ (mol m^{-3})	Number of experiments	Gz range	Average error (maximum error)[a] (%)	$120(D_B/D_A)$[b]	Average error (maximum error)[c] (%)
1	0.160	240	43.1	7	79–702	6.3 (8.9)	205	5.4 (7.3)
2	0.380	240	43.2	6	98–1080	7.3 (7.9)	205	4.3 (5.6)
3	0.165	500	43.1	7	40–473	7.4 (10.7)	212	5.9 (10.7)
4	0.165	950	43.1	7	23–386	9.1 (16.0)	226	6.2 (9.9)

Note: The percentage error is defined as $((E_{app,1} - E_{exp})/E_{app,1}) \times 100$.
[a] The maximum and average errors are based on $E_{app,1}$ calculated using $C_{B,0}$ or $C_{NaOH,0}$.
[b] Criterion for the applicability of approximate solution as per Eq. (35).
[c] The errors are based on $E_{app,1}$ calculated using $\langle C_B \rangle$ as per Eq. (34) instead of $C_{B,0}$.

Table 4
Experimental conditions for the data provided in the parity plot (continuous mode of operation)

Operating conditions	Numerical value
P (kPa)	103
T (K)	295
L (m)	0.33
d (m)	6.0×10^{-4}
$C_{NaOH,0}$ (mol m^{-3})	100
$C_{CO_2,g,in}$ (mol m^{-3})	2.58
Gz	173–1336

A limited number of experiments was also conducted in the continuous mode for which a gas stream (CO_2 in N_2) flowed outside the hollow fiber in the single fiber membrane contactor. These experiments were performed with the objective to obtain experimental data in regimes other than the instantaneous absorption regime for which experimental data were obtained in the semi-batch mode of operation. The experimental conditions are summarized in Table 4. Based on the conditions in the membrane contactor, the absorption is expected to be in the fast regime ($2 < Ha^* < E_\infty^*$). Since the concentration of CO_2 in the gas phase changes (though not significantly; <6% of $C_{CO_2,g,in}$) along the length of the hollow fiber, a log mean concentration ($C_{CO_2,g,LM}$) based on the inlet ($C_{CO_2,g,in}$) and outlet gas stream concentration ($C_{CO_2,g,out}$) was used in calculating the approximate infinite enhancement factor (E_∞^*). As $C_{CO_2,g,out}$ is unknown, it was estimated (along with $E_{app,1}$) iteratively as follows:

1. To start with, $C_{CO_2,g,out}$ was guessed and E_∞^* was calculated based on the $C_{CO_2,g,LM}$.
2. The average CO_2 absorption flux was calculated using Eq. (10), with the enhancement factor calculated using the adapted DeCoursey solution (Eq. (30)).
3. A mass balance over the gas phase provided a new value of $C_{CO_2,g,out}$.

The above steps were repeated till $C_{CO_2,g,out}$ converged. The values of the predicted enhancement factor along with the experimental values are also shown in the parity plot of Fig. 6. The maximum and average errors were 13.6 and 9.5% respectively. The somewhat larger error (in spite of the fact that the Graetz numbers studied are higher than that of the semi-batch measurements) for the continuous mode was expected because the k_L calculated from Leveque's solution assumes a constant gas–liquid interface concentration of A which is not true for the continuous experiments.

6.4. Influence of mass transfer resistance due to the microporous membrane

In the calculation of the experimental enhancement factor (E_{exp}) from the absorption flux measurements, the mass transfer resistances due to the gas phase ($1/k_g$) and microporous membrane ($1/k_m$) were neglected. Since pure CO_2 was used in the semi-batch measurements, the gas phase resistance can be neglected. Similarly, the gas phase resistance for the continuous measurements was minimized as described in Kumar et al. [9]. Depending upon the liquid side mass transfer resistance ($1/mk_LE$), the membrane resistance ($1/k_m$) can become significant. The pore diameter (d_p) of the polypropylene membrane used in the present work was relatively small (0.2 mm) and also the gas pressure was low. The membrane resistance was estimated for the continuous experiments. For the semi-batch experiments using pure gases, the resistance will be lower because, in that case, a concentration gradient across the microporous membrane can only be present if a pressure gradient is present. A pressure gradient (and the resulting convective flow) causes much larger CO_2 fluxes (than those measured in the semi-batch absorption experiments), and therefore, the possibility of a membrane resistance is unlikely in case pure gases are used for absorption.

The k_m for the continuous experiments (binary diffusion) was estimated simply using Eq. (4). The bulk diffusion coefficient was calculated from the kinetic theory of gases [26] and the Knudsen diffusion coefficient according to Eq. (6). The overall mass transfer coefficient was calculated from the experimental absorption flux as given below:

$$K_{ov,exp} = \frac{\langle J \rangle_{exp}}{mC_{CO_2,g}}$$

The estimated value of k_m was 4.62×10^{-2} m s^{-1} and the maximum value of $K_{ov,exp}$ for the continuous experiments was 1.07×10^{-3} m s^{-1}. Therefore the maximum contribution of the membrane resistance to the overall resistance is only 2.3%. Though the membrane does not offer any significant resistance for the present experiments, for a large enhancement

in absorption rate due to chemical reaction, the mass transfer resistance due to the membrane can become significant and has to be taken into account.

7. Conclusions

In this contribution, it was shown that approximate solutions for the enhancement factor, developed originally for mass transfer with chemical reaction in the presence of a well-defined liquid bulk can be adapted to situations where a liquid bulk may be absent and in addition a velocity gradient is present in the mass transfer zone. This was demonstrated using DeCoursey's explicit approximate solution for an irreversible second-order reaction as an example. For long gas–liquid contact time in a hollow fiber, the driving force for the gas phase species absorbed was found not to be identical for physical and reactive absorption. Therefore, an overall enhancement factor ($E_{app,l}$) was introduced for a proper basis of comparison with the exact numerical results.

The exact numerical results of the mass transfer model for a membrane fiber indicate that the approximate solution fails for very low values of the Graetz number due to a significant depletion of the liquid phase reactant at the axis of the hollow fiber (analogous to liquid bulk in traditional mass transfer models). For a second-order irreversible reaction, the use of approximate solutions is limited to $Gz > 120(D_B/D_A)$. Within the range of applicability, the approximate solutions were found to be very accurate in comparison to the exact numerical results as well as experimentally measured values of the enhancement factor. As shown with the experimental as well as numerical results, the approximate solution can be used for Graetz numbers lower than the above-mentioned criterion without a significant loss of accuracy. However, the error increases rather exponentially at very low values of the Graetz number.

The above prescribed lower limit for the Graetz number ($\langle v\rangle d^2/DL$) is a serious limitation in terms of the applicability of the approximate solution in the design of membrane gas–liquid contactors that use very small diameter hollow fibers (usually of the order of few hundred μm). The liquid velocity through these small diameter fibers is usually kept low to avoid a large pressure drop across the modules and therefore the operational Graetz numbers are usually lower than the prescribed criterion.

The absorption flux and enhancement factor measured in the single fiber membrane contactor, as described in this work and Kumar et al. [9] are very well predicted by the numerical model as well as the adapted DeCoursey's approximate solution. Since the hydrodynamics of the liquid flowing inside the hollow fiber of a single fiber membrane contactor is well defined (like in a laminar jet or wetted wall column), it can be used also as a model gas–liquid contactor. The approximate solutions for the enhancement factor can then be conveniently used to interpret the experimental absorption data to estimate the physicochemical or kinetic parameters for a reactive gas–liquid system. Conversely, if the above parameters are known from independent measurements, their accuracy can be independently verified by comparing the absorption fluxes predicted using the approximate solutions and the experimental absorption data, as was done in this work as well as that of Kumar et al. [9].

Acknowledgements

This research is part of the research programme carried out within the Centre for Separation Technology, a cooperation between the University of Twente and TNO, The Netherlands Organization for Applied Scientific Research. We acknowledge Wim Leppink for the construction of experimental setup.

References

[1] A. Gabelman, S. Hwang, Hollow fiber membrane contactors, J. Membr. Sci. 159 (1999) 61–106.
[2] A.L. Kohl, R.B. Nielsen, Gas Purification, 5th ed., Gulf Publishing Company, Houston, 1997.
[3] Z. Qi, E.L. Cussler, Microporous hollow fibers for gas absorption. II. Mass transfer across the membrane, J. Membr. Sci. 23 (1985) 333–345.
[4] S. Nii, H. Takeuchi, K. Takahashi, Removal of CO_2 by gas absorption across a polymeric membrane, J. Chem. Eng. Jpn. 25 (1) (1992) 67–72.
[5] D.W. van Krevelen, P.J. Hoftijzer, Kinetics of gas–liquid reactions. I. General theory, Rec. Travel Chim. 67 (1948) 563–586.
[6] S. Nii, H. Takeuchi, Removal of CO_2 and/or SO_2 from gas streams by a membrane absorption method, Gas Sep. Purif. 8 (2) (1994) 107–114.

[7] K. Li, W.K. Teo, Use of permeation and absorption methods for CO_2 removal in hollow fiber membrane modules, Sep. Purif. Technol. 13 (1998) 79–88.
[8] H. Kreulen, C.A. Smolders, G.F. Versteeg, W.P.M. van Swaaij, Microporous hollow fiber membrane modules as gas–liquid contactors. Part 2. Mass transfer with chemical reaction, J. Membr. Sci. 78 (1993) 217–238.
[9] P.S. Kumar, J.A. Hogendoorn, P.H.M. Feron, G.F. Versteeg, New absorption liquids for the removal of CO_2 from dilute gas streams using membrane contactors, Chem. Eng. Sci. 57 (9) (2002) 1639–1651.
[10] K.R. Westerterp, W.P.M. van Swaaij, A.A.C.M. Beenackers, Chemical Reactor Design and Operation, Wiley, New York, 1984.
[11] A.A. Yeramian, J.C. Gottifredi, J.J. Ronco, Mass transfer with homogenous second order irreversible reaction. A note on an explicit expression for the reaction factor, Chem. Eng. Sci. 25 (1970) 1622–1624.
[12] H. Hikita, S. Asai, Gas absorption with (*m*, *n*)-th order irreversible chemical reaction, Int. J. Chem. Eng. 4 (1964) 332–340.
[13] K. Onda, E. Sada, T. Kobayashi, M. Fujine, Gas absorption accompanied by complex chemical reaction. I. Reversible chemical reactions, Chem. Eng. Sci. 25 (1970) 753–760.
[14] W.J. DeCoursey, Absorption with chemical reaction: development of a new relation for the Danckwerts model, Chem. Eng. Sci. 29 (1974) 1867–1872.
[15] W.J. DeCoursey, Enhancement factor for gas absorption with reversible chemical reaction, Chem. Eng. Sci. 37 (1982) 1483–1489.
[16] M. Mulder, Basic Principles of Membrane Technology, Kluwer Academic Publishers, Dordrecht, The Netherlands, 1996.
[17] C.M. Guijt, I.G. Racz, T. Reith, A.B. de Haan, Determination of membrane properties for use in the modelling of a membrane distillation module, Desalination 132 (2000) 255–261.
[18] J. Leveque, Les Lois de la Transmission de Chaleur par Convection, Annals Mines, Series 12, Paris, 1928, p. 201.
[19] H. Kreulen, C.A. Smolders, G.F. Versteeg, W.P.M. van Swaaij, Microporous hollow fiber membrane modules as gas–liquid contactors. Part 1. Physical mass transfer processes, J. Membr. Sci. 78 (1993) 197–216.
[20] G.F. Versteeg, J.A.M. Kuipers, F.P.M. van Beckum, W.P.M. van Swaaij, Mass transfer with complex reversible chemical reactions. I. Single reversible chemical reaction, Chem. Eng. Sci. 44 (1989) 2295–2310.
[21] W.J. DeCoursey, R.W. Thring, Effects of unequal diffusivities on enhancement factors for reversible and irreversible reaction, Chem. Eng. Sci. 44 (8) (1989) 1715–1721.
[22] J.A. Hogendoorn, R.D. Vas Bhat, J.A.M. Kuipers, W.P.M. van Swaaij, G.F. Versteeg, Approximation for the enhancement factor applicable to reversible reactions of finite rate in chemically loaded solutions, Chem. Eng. Sci. 52 (24) (1997) 4547–4559.
[23] R.M. Secor, J.A. Beutler, Penetration theory for diffusion accompanied by a reversible chemical reaction with generalized kinetics, AIChE J. 13 (1967) 365–373.
[24] G.F. Versteeg, W.P.M. van Swaaij, Solubility and diffusivity of acid gases (CO_2, N_2O) in aqueous alkanolamine solutions, J. Chem. Eng. Data 33 (1988) 29–34.
[25] E.P. van Elk, Gas–liquid reactions: influence of liquid bulk and mass transfer on process performance, Ph.D. Thesis, University of Twente, The Netherlands, 2001.
[26] R.C. Reid, J.M. Prausnitz, B.E. Poling, The Properties of Gases and Liquids, McGraw-Hill, Singapore, 1987.
[27] S. Weisenberger, A. Schumpe, Estimation of gas solubilities in salt solutions at temperatures from 273 to 363 K, AIChE J. 42 (1996) 298–300.
[28] H. Hikita, S. Asai, T. Takatsuka, Absorption of carbon dioxide into aqueous sodium hydroxide and sodium carbonate–bicarbonate solutions, Chem. Eng. J. 11 (1976) 131–141.
[29] A.L. Hovarth, Handbook of Aqueous Electrolytic Solutions: Physical Properties, Estimation and Correlation Methods, Wiley, New York, 1985.
[30] R. Pohorecki, W. Moniuk, Kinetics of the reaction between carbon dioxide and hydroxyl ion in aqueous electrolyte solutions, Chem. Eng. Sci. 43 (1988) 1677–1684.